

# Non-linear modeling of masonry churches through a discrete macro-element approach

Bartolomeo Pantò<sup>\*1</sup>, Linda Giresini<sup>2a</sup>, Mauro Sassu<sup>3b</sup> and Ivo Calió<sup>1c</sup>

<sup>1</sup>Department of Engineering and Architecture, University of Catania, Viale A. Doria 6 - 95125 Catania, Italy

<sup>2</sup>Department of Energy Systems Territory and Construction Engineering, University of Pisa, Largo Lucio Lazzarino - 56122 Pisa, Italy

<sup>3</sup>Department of Civil, Environmental Engineering and Architecture, University of Cagliari, Via Marengo 2, 09123 Cagliari, Italy

(Received July 26, 2016, Revised January 26, 2017, Accepted January 26, 2017)

**Abstract.** Seismic assessment and rehabilitation of Monumental Buildings constitute an important issue in many regions around the world to preserve cultural heritage. On the contrary, many recent earthquakes have demonstrated the high vulnerability of this type of structures. The high nonlinear masonry behaviour requires ad hoc refined finite element numerical models, whose complexity and computational costs are generally unsuitable for practical applications. For these reasons, several authors proposed simplified numerical strategies to be used in engineering practice. However, most of these alternative methods are oversimplified being based on the assumption of in-plane behaviour of masonry walls. Moreover, they cannot be used for modelling the monumental structures for which the interaction between plane and out-of-plane behaviour governs the structural response. Recently, an innovative discrete-modelling approach for the simulation of both in-plane and out-of-plane response of masonry structures was proposed and applied to study several typologies of historic structures. In this paper the latter model is applied with reference to a real case study, and numerically compared with an advanced finite element modelling. The method is applied to the St. Venerio church in Reggiolo (Italy), damaged during the 2012 Emilia-Romagna earthquake and numerically investigated in the literature.

**Keywords:** cultural heritage; monumental; structures; masonry churches; macro-element approach; discrete element approach; non-linear finite element model; seismic vulnerability; HiStrA software; ABAQUS software

## 1. Introduction

In the literature, the numerical modelling of monumental buildings was faced using several approaches. The simplest one consists of a kinematic analysis for which the structure is divided in independent sub-elements (*macro-elements*), such as façades, apses, triumphal arches and vaults in churches, and a limit analysis is performed for each identified collapse mechanism. The concept of macro-element was first introduced by Doglioni *et al.* (1994) and used to analyze the behavior of masonry portal frames or arches (De Luca *et al.* 2004). In addition to the kinematic approach, a rocking analysis can be effectively applied to study these elements in a dynamic perspective (Giresini *et al.* 2016, Giresini and Sassu 2016), also by identifying ground motions that can cause ‘rocking resonance’ (Casapulla *et al.* 2010, Casapulla 2015). The macro-element approach, based on the Heyman’s hypotheses (Heyman

1999), is useful when there are uncertainties in the definition of the masonry mechanical properties and/or a simplified analysis has to be performed. By following a macro-element approach, the non-linear state of the structure could be represented by means of macroscopic state parameters, such as the dissipated energy related to each macro-element identified collapse mechanism (Giresini 2015). Nevertheless, where the mechanical and geometrical properties are known (Rovero *et al.* 2016), more sophisticated approaches for the seismic vulnerability assessment are available. Among them, nonlinear finite elements can be employed aiming at reproducing the degrading nonlinear cyclic behaviour of masonry (Asteris *et al.* 2014), both in static and dynamic fields. In the last decade many contributions by several authors investigated the capability and the performances of the advanced numerical tools based on refined finite element (FE) approaches on the seismic assessment of complex historical and monumental buildings, whose response is strongly conditioned by the interaction between the in-plane and out-of-plane behaviors (Lourenço *et al.* 2011, Mendes and Lourenço 2010, Lourenço *et al.* 2012, Betti e Vignoli 2012, Betti and Vignoli 2011, Barbieri *et al.* 2013). An alternative approach to the non-linear FEM is represented by the rigid-body spring models (RBSM), specifically formulated with the aim of approximating the macroscopic behaviour of masonry walls with a reduced amount of degrees of freedom (Casolo and Sanjustb 2009).

A particular typology of monumental structures is

\*Corresponding author, Ph.D.

E-mail: [bpanto@dica.unict.it](mailto:bpanto@dica.unict.it)

<sup>a</sup>Ph.D.

E-mail: [linda.giresini@unipi.it](mailto:linda.giresini@unipi.it)

<sup>b</sup>Professor

E-mail: [msassu@unica.it](mailto:msassu@unica.it)

<sup>c</sup>Professor

E-mail: [icalio@dica.unict.it](mailto:icalio@dica.unict.it)

represented by churches and monasteries. A wide literature on the numerical modelling of such structures is available. The studies regard both the seismic vulnerability assessment and the numerical simulation of the consequent retrofit (Lourenço *et al.* 2001, Moropoulou *et al.* 2003, Lourenço *et al.* 2007, Lourenço *et al.* 2008, Araujo *et al.* 2012). Recent studies have investigated several typologies of masonry churches damaged by earthquake events by using static pushover analyses and limit analyses (Milani and Valente 2015a, b) in order to numerically simulate partial and global failure mechanisms and to evaluate the performance level associated with their activation. However, the latter approaches require sophisticated constitutive laws and a huge computational cost to perform the analyses. Furthermore advanced skills are needed for model implementation and interpretation of the results; this effort is often not compatible with practical engineering applications.

For these reasons, in the last decades several simplified theoretical models were proposed by different research teams, as an alternative to the finite element, for predicting the nonlinear seismic behaviour of unreinforced masonry structures, particularly for buildings. A review on the state of the art on the existing simplified approaches for the seismic assessment of unreinforced masonry building has been provided by Marques and Lourenço (2011), who performed a critical comparison among different numerical strategies. However, most of the simplified methods, currently available in the literature, are not suitable to simulate the response of monumental buildings, since they embed the strong limit of a 2D kinematics. Recently, an original 3D macro-model approach, able to simulate the nonlinear behavior of masonry churches and, more in general, of complex monumental structures, was proposed by Pantò *et al.* (2016). This model has been obtained as an evolution of a 2D discrete macro-element originally conceived for the simulation of unreinforced masonry buildings with box behavior (Caliò *et al.* 2012). Subsequently, it was adapted to model the in-plane behaviour of mixed reinforced concrete masonry structures, such as confined masonry and infill frame (Caliò and Pantò 2014) and implemented in the program 3DMacro (2014). The program was then employed for further validations based both on numerical and experimental results (Marques and Lourenço 2014).

The 3D spatial model can be represented by means of an equivalent simple mechanical scheme, as described in Pantò *et al.* (2016) and summarized in Section 2. The model kinematic is characterized by seven Lagrangian parameters. In spite of its simplicity the model is capable of simulating the out-of-plane behavior of plane and curved sub-structures (Caddemi *et al.* 2015) and, for assemblage, entire complex monumental structures (Caddemi *et al.* 2014). This theoretical model has been implemented in the software “HiStrA” employed both in engineering and research purposes (HiStrA software 2015).

A relevant improvement of the proposed methodology will consist in extending the model to simulate the out-of-plane behaviour of infilled frame structures. With this aim, a new interface element, able to reproduce the detachment

and the sliding between the infill and the surrounding frame in a tridimensional context, will be introduced.

In the paper, with the aim of showing a detailed and critical numerical comparison between the discrete modelling approach and the more refined finite element approach, a single-nave church, severely damaged by the Italian 2012 earthquake, is analyzed by using both procedures. The study has been performed according to three different stages:

- comparison in the linear field by means of modal analysis;

- comparison in the non-linear field by means of a parametric analysis to assess the influence of non-linear mechanical properties on the response of isolated walls.

- comparison of nonlinear numerical simulations of the entire church by expressing the results in terms of capacity curves and failure mechanisms to verify the mechanical consistency between the discrete macro-model and the continuous FEM model.

The obtained results seem to confirm the capability of the proposed discrete model approach to be applied for the seismic assessment of monumental structures.

## 2. The 3D macro-model for modelling monumental buildings

The three dimensional discrete element, proposed in Pantò *et al.* (2016), represents an upgrade of a plane macro-element introduced by Caliò *et al.* (2012) for the simulation of the in-plane nonlinear response of masonry walls. The plane macro-element consists of a pinned quadrilateral made with four rigid edges, in which a nonlinear diagonal link is connected to the corners to simulate the shear response. Each side of the panel can interact with other panels, elements or supports by means of a discrete distribution of nonlinear springs, denoted as interface. Each interface is constituted by a single row of  $n$  nonlinear springs, orthogonal to the panel side, and an additional longitudinal spring, which rules the relative motion in the direction of the panel edge, Fig. 1(a).

In the three-dimensional macro-element, Fig. 1(b), several nonlinear transversal rows of transversal links were introduced in order to account for the three-dimensional mechanical behaviour of the element according to a discrete fiber discretization strategy. The kinematics of the spatial macro-element is governed by 7 degrees-of-freedom: 4 in

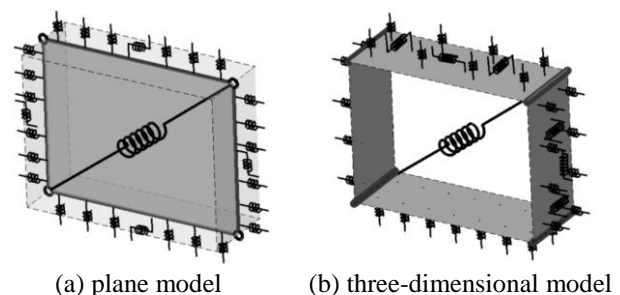
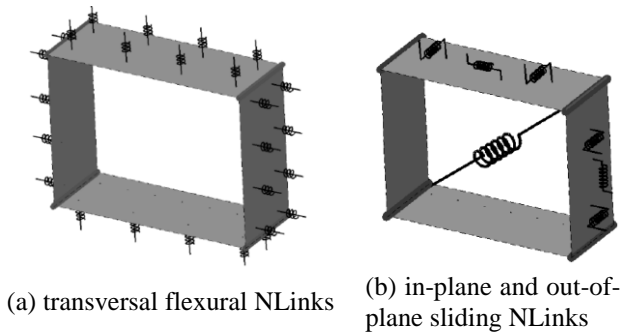


Fig. 1 Geometrical scheme of the discrete macro element



(a) transversal flexural NLinks (b) in-plane and out-of-plane sliding NLinks  
 Fig. 2 Mechanical representation of the three-dimensional macro-element

the in-plane behaviour including the plane shear deformability and 3 degrees-of-freedom for the out of plane rigid body motions.

The interaction of the spatial macro-element with the adjacent elements or the external supports is ruled by 3D-interfaces. Each 3D-interface possesses  $m$  rows of  $n$  longitudinal (i.e., perpendicular to the planes of the interface) NLinks. Consequently, each interface is discretized, similarly to what is done in classical fiber models, in  $m \times n$  sub-areas (Fig. 2(a)). Besides the interface orthogonal springs, the 3D interfaces are endowed with additional transversal sliding springs (Fig. 2(b)). The latter are required to control the in-plane and out-of plane sliding mechanisms and the torsion around the axis perpendicular to the plane of the interface. The shear deformation is ruled by a single non linear spring placed along one of the diagonals of the articulated quadrilateral (Fig. 2(b)).

The great importance of the stabilising role of friction between interlocked elements was recently highlighted in comparison with other extrinsic or intrinsic loading capacities for in-plane and out-of-plane failure modes (Casapulla and Argiento 2016).

Each macro-element must be representative of the corresponding finite portion of masonry wall by imposing simple mechanical equivalence procedures, based on the main macroscopic mechanical parameters of masonry, according to an orthotropic homogeneous medium. The mechanical characterization of the model, that relies on the definition of the constitutive laws of the nonlinear links, is described more in detail in Calìo *et al.* (2012). In the simulations, reported in the following section, an elastoplastic behaviour has been considered for the orthogonal links of the interfaces with limited ductility, governed by a fractural energy criterion. The Mohr-Coulomb criterion was assumed for the sliding nonlinear links, while the Turnsek and Cacovic criterion Calìo *et al.* (2012) was considered for the diagonal shear link. For a panel of length  $l$  and thickness  $t$ , subjected to compression and shear, the latter criterion can be expressed as reported in the following Eq. (1), where  $f_{v0}$  is the average shear strength in the wall in absence of compression;  $\sigma$  is the average compression stress due to vertical load  $N$  divided by the transversal area ( $l \times t$ ).

$$V_u = l \cdot t \left[ f_{v0} \sqrt{1 + \frac{\sigma}{1,5 f_{v0}}} \right] \quad (1)$$

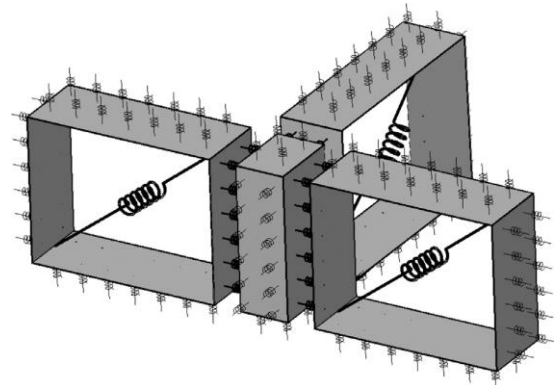


Fig. 3 Modeling strategy of the connections between orthogonal walls (from Pantò *et al.* 2016)

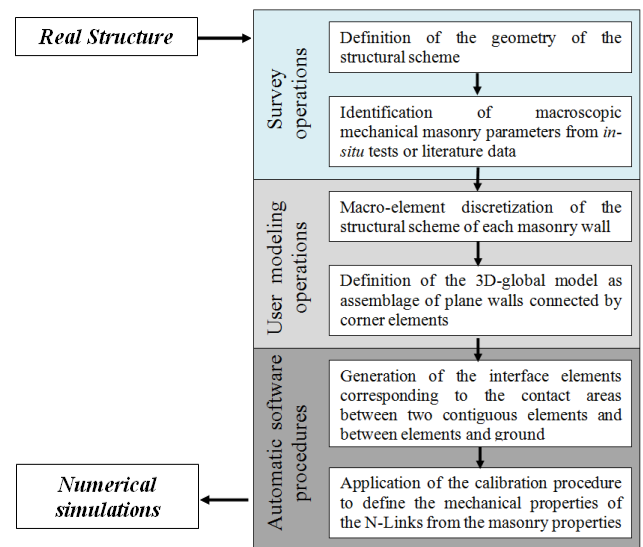


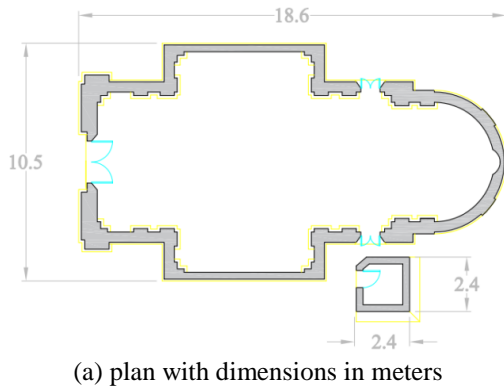
Fig. 4 Flow-chart of the modeling procedure by means of the discrete macro-model

The intersections between the orthogonal walls are modelled by means rigid elements connected with the panels by means of discrete interfaces (Fig. 3). More details can be found in Pantò *et al.* (2016).

An important aspect, for the applicability of the proposed method to real applications, is the complete automation, in the software HiStrA, of the generation of interface elements. These elements correspond to the contact areas between two continuous elements and between the elements and the ground. Furthermore the automatic calibration procedures allow to characterize the non-linear links from the macroscopic masonry mechanical properties, according to a user-defined level of discretization. A synthetic flow-chart, reported in Fig. 4, shows the main steps needed to obtain the global discrete-element model, starting from the geometrical and mechanical parameters of the structure.

### 3. The considered case study: San Venerio church damaged by 2012 Emilia Earthquake

St Venerio church is located in Via Roma, Reggiolo



(a) plan with dimensions in meters



(b) north-eastern façade

Fig. 5 St. Venerio church

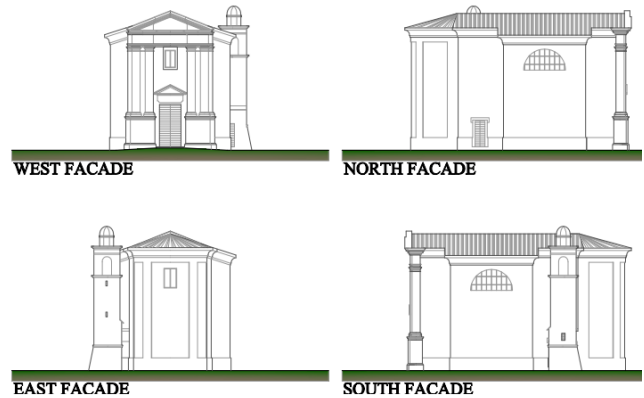


Fig. 6 Façades of the church



(a) Overturning mechanism (b) in-plane failure of the main façade

Fig. 7 Failure and damage mechanisms

(Emilia Romagna region, Italy), 20 km far from the epicenter of the earthquake that struck the Emilia Romagna Italian region on 2012 May, 29<sup>th</sup> (Andreini *et al.* 2014). After some constructive stages started in the 11<sup>th</sup> century, the structure was rebuilt at the end of 18<sup>th</sup> century.

The building is structurally isolated and has a plan inscribed in a rectangle of 18.6×10.5 m (Fig. 5). The main neo-classic façade is oriented to north-west and has a maximum height of 11 m (Fig. 6). The bell tower has plan-dimensions of 2.4×2.4 m and is structurally independent from the building. An “in folio” clay units semi spherical and 6-cm thick dome covers in the central part of the nave. Seven masonry arches, five of them strengthened by the presence of iron tie-rods, are located at four sides of the structure. The masonry roofs (vaults and arches) are constituted by an in-folio disposal (thickness about 6-10 cm). The thickness of the vertical walls depends on the façade: the main façade is 70 cm-thick, the longitudinal walls with the lunettes are 30 cm-thick, whereas the remaining walls have a thickness of 45 cm.

The church is entirely built with clay bricks and lime mortar, often used in the nearby area for similar historic chapels; the clay units have dimensions 32×16×6 cm.

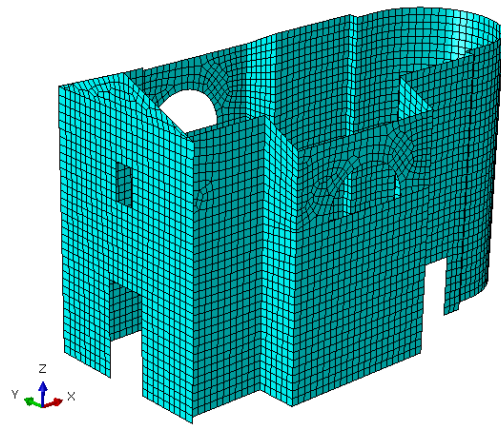
The 2012 Emilia earthquake caused severe damages to the church: the timber roof and the main vault partially collapsed, an partial overturning mechanism of the main façade and the apse occurred and out-of-plane and in-plane damages were observed in the façades (Fig. 7). The damage scenarios are described more in detail by Giresini (2015).

### 3.1 The Finite Element model of the church

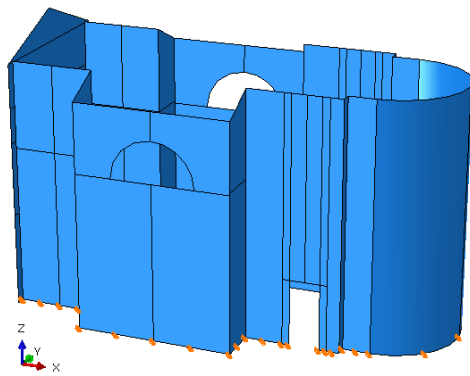
The entire church was modelled in ABAQUS CAE 6.12 (Simulia Abaqus 2014). The model counts 19.156 nodes, 6.210 quadratic quadrilateral elements of type S8R and 13 quadratic triangular elements of type STRI65 (Fig. 8(a)). The translations in X, Y, Z are set to zero at the base nodes (Fig. 8(b)). The total mass of the model is 429.8 tons. The arches, vaults and timber roof are not modelled for the sake of simplicity, given that a numerical comparison has to be performed. The non-linear material model used in the finite element program ABAQUS is the Concrete Damaged Plasticity (Abaqus 2014). For more details on the finite element model the reader is referred to Giresini (2015).

### 3.2 The Discrete element model of the church

The discrete model is developed by using an average mesh size of about 50 cm, larger than the mesh size used for the FEM. It is made of 1980 quadrilateral shear deformable elements, 20 triangular shear rigid elements and 4486 interfaces. Furthermore, 180 solid elements are used to connect the walls at the corners and the façade to the two longitudinal walls. The model has a total of 15.060 degrees of freedom. Fig. 9 shows 3D view and 2D lateral view of the discrete model implemented in the software HiStrA (2015).

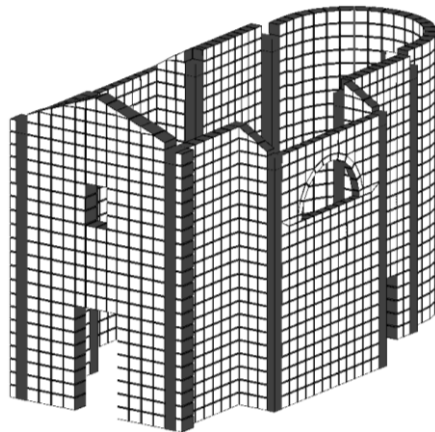


(a) mesh discretization

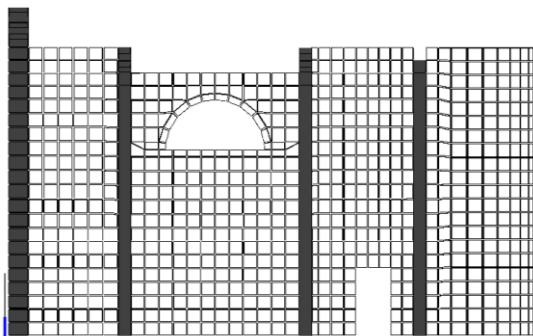


(b) boundary conditions of the native model

Fig. 8 Finite Element model



(a) 3D view



(b) 2D view of longitudinal wall

Fig. 9 Discrete Macro model element mesh

Table 1 Computational parameters associated to the finite continuous model and the discrete model

	Number of elements	Degrees of freedom	Number of control points
Finite element model	6223	114936	49784
Discrete model	2180	15060	6460
Ratio [%]	35,03	13,10	12,98

The model discretization has been chosen with the aim of obtaining satisfactory results through a parsimonious model of the entire church, i.e., characterized by a reduced number of computational elements and degrees of freedom, if compared to a reliable non-linear FEM model. In order to estimate the reduction of the computational effort by means of the discrete model, in Table 1 the main global computational parameters are reported for the finite element model and the discrete model. Furthermore, the reduction ratio between the value related to the discrete model and the value related to the finite element model is reported in the third row of the Table. In addition to the number of elements and the number of the degrees of freedom, a comparison in terms of “control points” is specified in the third column. For the continuous model the control points correspond to the Gauss points (8 for each element), in which the stress state is evaluated to determine the plastic events. In the macro modeling approach, analogously to the fiber beam fiber models, the control points can be identified with the interface elements and the internal diagonal shear springs within the quadrilateral elements. A strong reduction rate of the computational indices can be observed. In particular, a reduction of 87% in terms of the global degrees of freedom results. This is a key aspect because this parameter is directly related to the effort needed to impose the global equilibrium of the structure, at each step of the analysis.

#### 4. Comparison in terms of linear dynamic properties

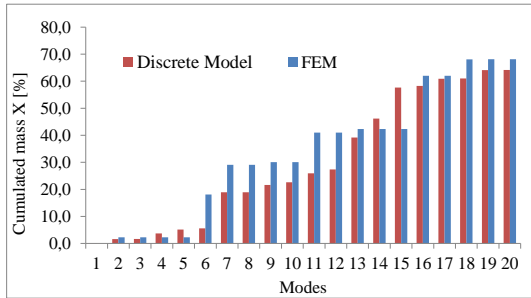
In this paragraph, the capability of the discrete modelling approach to predict the eigen properties of the structure is discussed. To this aim, modal analysis is carried out for the two different numerical models, assuming a linear elastic behaviour. The traditional finite element model is described in Section 3.1, whereas the discrete model is illustrated in Section 3.2. It is worthy to notice that two different mesh size discretizations were considered. For the continuous FEM model an average size of 20 cm was used in the mesh resolution with the aim to obtain accurate results both in linear and non-linear context and to obtain a satisfactory description of the damage path during the push-over analyses, reported in the next section. On the contrary, a larger mesh discretization (an average size of 50 cm) was used for the discrete model according to the philosophy of the macro-element approach. Moreover, this investigates the capability of the model of properly simulating the mechanical behaviour by using a larger mesh compared to the standard accepted for the continuous models with a

drastic reduction of degrees of freedom (parsimonious model). The linear deformation modulus of the masonry in normal direction ( $E=1200$  Mpa) and in the tangential direction ( $G=480$  Mpa), as well as the weight density ( $w=18$  kN/m<sup>3</sup>) are chosen according to literature data and technical guidelines (NTC 2008, Explanatory circular 617 2009) with references to the masonry material of the church.

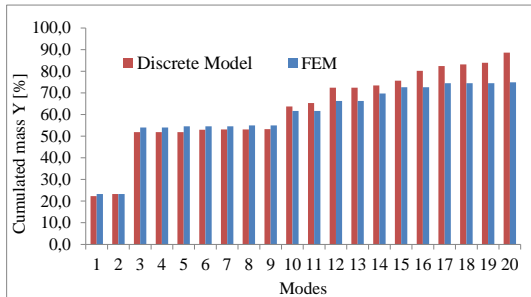
The first twenty periods with the effective mass ratios and cumulated masses, along the longitudinal direction (X) and the transversal direction (Y), are listed in Fig. 10 for both FEM model and discrete model.

Modes	Discrete model					FEM				
	Period [sec.]	Mx [%]	My [%]	Σ Mx [%]	Σ My [%]	Period [sec.]	Mx [%]	My [%]	Σ Mx [%]	Σ My [%]
1	0,41	0,1	22,3	0,1	22,3	0,43	0,0	23,3	0,0	23,3
2	0,41	1,5	1,0	1,6	23,3	0,42	2,3	0,0	2,3	23,3
3	0,27	0,1	28,6	1,7	51,9	0,28	0,0	30,7	2,3	54,0
4	0,25	2,0	0,0	3,7	51,9	0,25	0,0	0,0	2,3	54,0
5	0,24	1,5	0,0	5,2	51,9	0,24	0,0	0,6	2,3	54,6
6	0,24	0,4	1,1	5,6	53,0	0,22	15,8	0,0	18,1	54,6
7	0,20	13,4	0,1	19,0	53,1	0,20	11,0	0,0	29,1	54,6
8	0,19	0,0	0,0	19,0	53,1	0,19	0,0	0,4	29,1	55,0
9	0,16	2,7	0,1	21,6	53,2	0,16	1,0	0,0	30,1	55,0
10	0,16	1,0	10,5	22,7	63,7	0,16	0,0	6,7	30,1	61,7
11	0,15	3,3	1,6	25,9	65,3	0,15	10,9	0,0	41,0	61,7
12	0,15	1,4	7,2	27,4	72,5	0,14	0,0	4,6	41,0	66,3
13	0,13	11,8	0,0	39,2	72,5	0,14	1,3	0,0	42,3	66,3
14	0,13	7,0	1,0	46,2	73,5	0,14	0,0	3,4	42,3	69,7
15	0,12	11,5	2,2	57,6	75,7	0,13	0,0	2,9	42,3	72,6
16	0,12	0,6	4,5	58,2	80,2	0,13	19,7	0,0	62,0	72,6
17	0,12	2,7	2,2	60,9	82,4	0,1199	0,0	1,9	62,0	74,5
18	0,1	0,2	0,8	61,0	83,2	0,1097	6,1	0,0	68,1	74,5
19	0,1	3,1	0,7	64,1	83,9	0,1056	0,0	0,0	68,1	74,5
20	0,1	0,1	4,7	64,2	88,6	0,1054	0,0	0,4	68,1	74,9

(a) periods of vibration and modal mass ratios

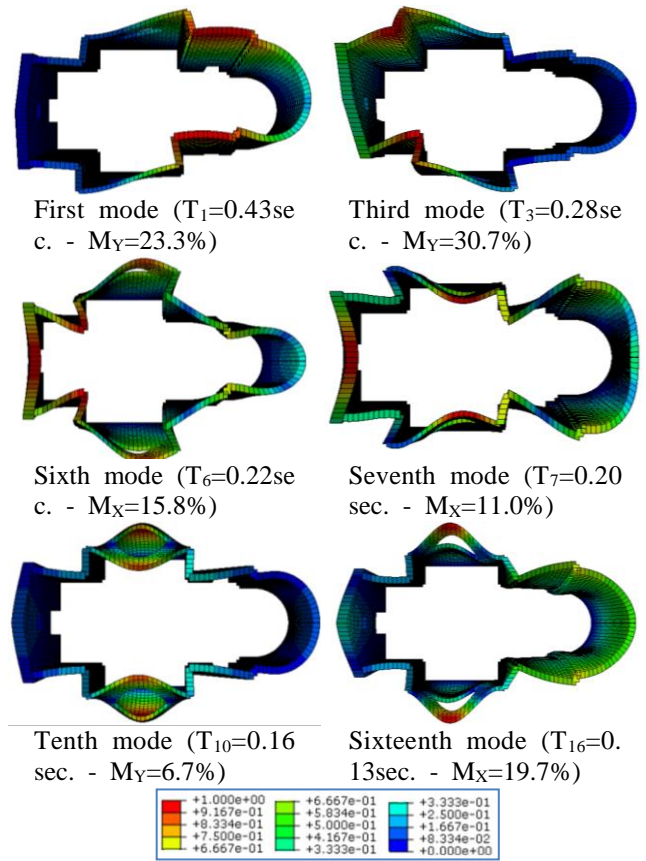


(b) modal mass cumulated in X direction

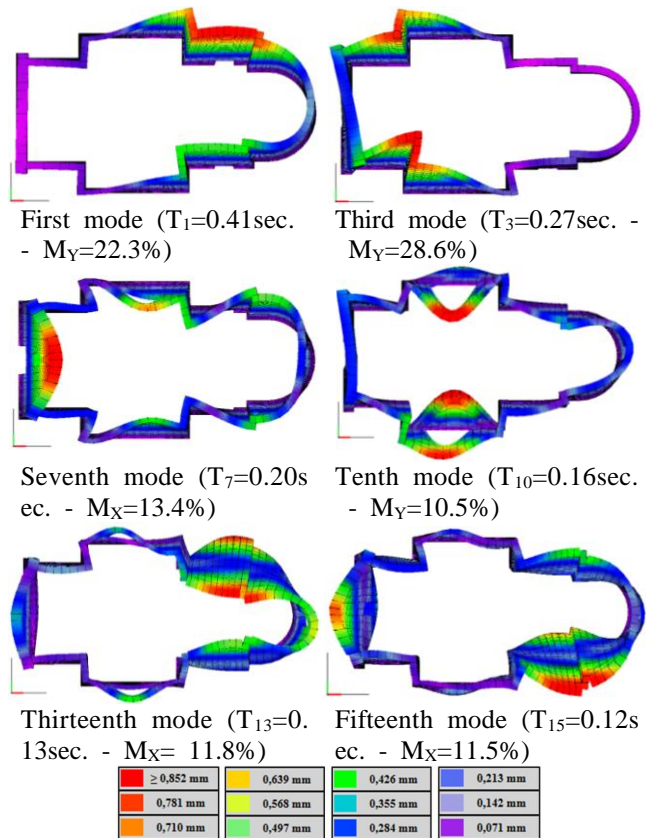


(c) modal mass cumulated in Y direction

Fig. 10 Comparison between discrete and continuous model in the linear field



Magnitude displacement (mm)  
Fig.11 Modes shape of FEM model



Magnitude displacement (mm)

Fig. 12. Modes shape of discrete model

Fig. 11 displays the first six modes of vibration of the continuous model, in terms of effective mass activated. The corresponding mode shapes obtained by the discrete model are shown in Fig. 12.

A very good agreement can be observed between the two models, both in terms of natural frequencies and mode shapes of vibration. In addition, the distribution of the effective modal masses, associated with each mode shape of vibration, are in great agreement in the two different adopted discretizations.

These results allow concluding that the proposed discrete macro model is able to simulate the linear dynamic properties of the structure at significant lower computation cost than the FEM model.

### 5. Characterization of the masonry non-linear mechanical properties and parametric investigation

The parameters that govern the masonry mechanical behaviour were coherently assigned in the two models. Preliminary tests on isolated masonry walls, loaded in their plane, have been performed in order to verify the correspondence between the discrete and the finite element models and with the aim to investigate the sensitivity of the non-linear response of the two models on the variability of the main mechanical parameters. The masonry non-linear properties were defined by using an elasto-plastic behaviour governed by the ultimate compression strength ( $f_c$ ) and the ultimate tensile strength ( $f_t$ ). The ductility was governed by means of fractural energy, in tensile ( $g_t$ ) and compression ( $g_c$ ). Limited to the discrete model, independent parameters are necessary to govern the diagonal shear mechanism. In particular, the shear strength in absence of axial compression ( $f_{v0}$ ), used in the Cacovic criterion (1), and the ultimate shear deformation ( $\gamma_u$ ) have to be defined.

In order to guarantee a mechanical coherence between the discrete and continuous model,  $f_{v0}$  was fixed equal to the tensile strength  $f_t$ , and the shear ductility was determined according to the masonry fractural energy by using the relation  $\gamma_u = g_t / (L f_{v0})$ , being  $L$  is mesh size.

In the discrete model a mesh discretization with size of 50 cm is used, while a more refined mesh is adopted for the finite element model (15 cm). The aim is to evaluate the capability of the macro model of properly simulating the non-linear response of the panel with a reduced computational effort. However, a sensitivity analysis is numerically performed and the results are reported in the following. Nevertheless, more detailed sensitivity analyses on the influence of the mesh size are reported in (Caddemi *et al.* 2015) and (Pantò *et al.* 2016).

Since no experimental tests are available for the masonry under examination, the non linear mechanical parameters have been chosen according to the indications of the Italian code for existing buildings, considering the masonry typology composed by clay bricks and mortar joints (NTC 2008, Explanatory circular 617 2009). The reference values of the masonry mechanical parameters are summarized in Table 2.

The first parametric analysis has been performed with

the aim to investigate the flexural behaviour by considering a wall fully restrained at the base and free at the top section, with dimensions  $150 \times 300 \times 30 \text{ cm}^3$  (*cantilever wall*). Two different models are considered by changing the tensile fractural energy: the first model is representative of a ductile masonry (*cantilever 1*) with  $g_t = 0.15 \text{ N/mm}$ ; and the second model (*cantilever 2*), with  $g_t = 0.015 \text{ N/mm}$  is representative of brittle masonry.

The results, in terms of collapse mechanisms, are displayed in Fig. 13 in which the deformed shape at the last step of the analysis, of the brittle models, are reported with the corresponding distributions of damage. In particular, Fig. 13(a) shows the damage distribution of the FEM model. For the discrete model the plastic deformation ratio ( $\epsilon_p / \epsilon_{pu}$ ) between the normal plastic deformation ( $\epsilon_p$ ) and the ultimate plastic deformation ( $\epsilon_{pu}$ ), relative to the transversal links of interfaces, is represented by a grey scale representation (Fig. 13(b)). The latter is easily correlated with the plastic cumulated energy.

Moreover, Fig. 14(a) shows the comparison of the capacity curves and the limit analysis value (rigid body assumption). A very good correspondence between the two sets of numerical results can be observed, as the curves are characterized by the same trend with a residual shear strength asymptotically approaching to the value provided by the limit analysis. Furthermore, the influence of the mesh-size on the discrete model response is shown in Fig. 14(b), by considering three different mesh refinements: 50 cm, 25 cm and 10 cm. The responses of all the investigated models are in a good agreement with the response of the continuous model.

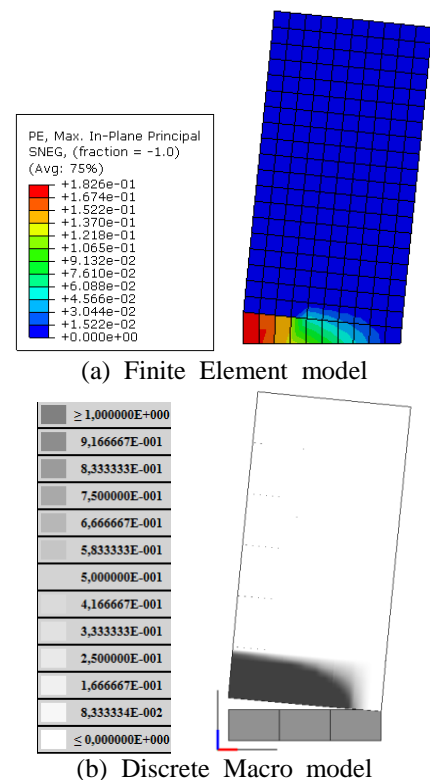


Fig. 13. Isolated wall (Cantilever 2): deformed shape and plastic deformation distribution

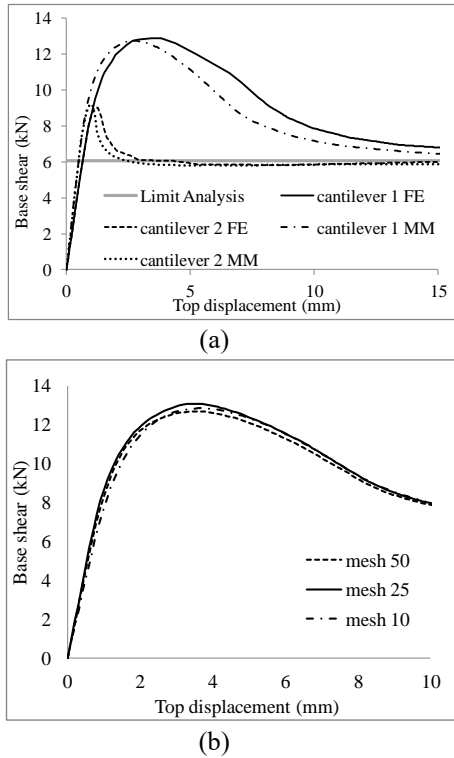


Fig. 14 Cantilever wall: (a) comparison of capacity curves between FEM model and discrete model; (b) sensitive analysis on the mesh-size of the discrete macro-model

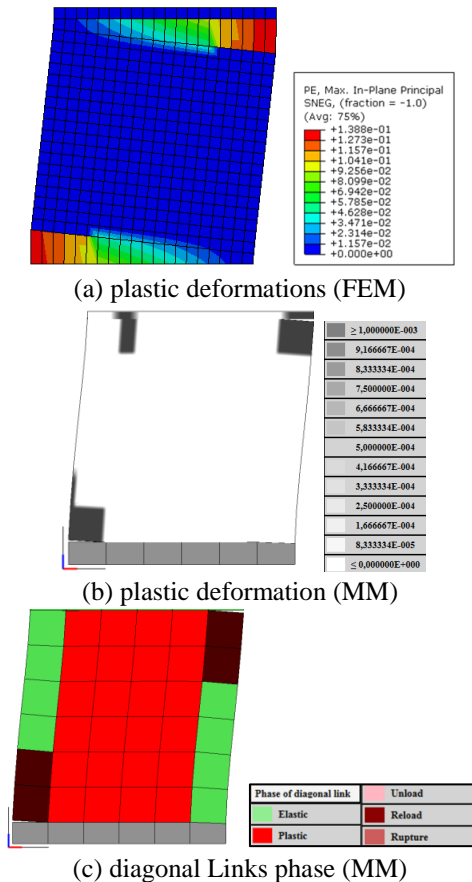


Fig. 15 Simulation of the shear collapse of the continuous model (FEM) and the macro model (MM)

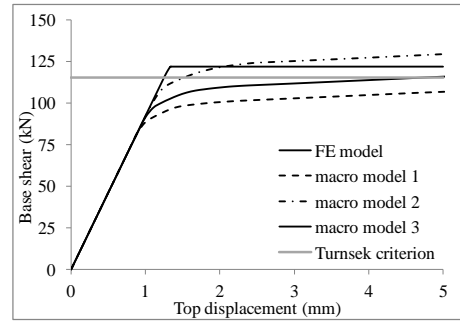


Fig. 16 Comparison of the shear response: comparison between continuous and discrete model

Table 2 Mechanical parameters considered in the analyses of the isolated wall

E	$f_c$	$f_t$	$g_c$	$g_t$	G
[MPa]	[MPa]	[MPa]	[N/mm]	[N/mm]	[MPa]
1200	2.40	0.1	Not limited	0.015	480

Table 3 Models considered in the sensitive analyses on flexural mechanical parameters on isolated wall

Model	model 1	model 2	model 3
$f_i/f_{i0}$	1.50	1.25	1.00
$f_{v0}$ [Mpa]	0.067	0.080	0.100

The second numerical investigation has been performed with the aim to verify the correspondence between the two models when the shear failure mechanism occurs. The analyses have been performed on a single wall with dimensions  $300 \times 300 \times 30 \text{ cm}^3$  fully restrained at the base and with fixed rotations at the top section, where a vertical compression load of 0.27 MPa is applied. Three different values of ratio  $f_i/f_{i0}$ , are considered, as reported in Table 3.

Fig. 15 reports the details on the damage scenarios corresponding to the last step of the analysis. In particular, Fig. 15(a) and Fig. 15(b) respectively display the normal plastic deformations registered in the discrete and in the continuous FE model, while Fig. 15(c) reports the shear yielding mechanisms of the diagonal *NLinks* of the discrete model. Fig. 16 shows the comparison in terms of capacity curve considering both numerical approaches and the theoretical criterion of Tusnsek and Cacovic (1). It can be observed that the model 3, in which  $f_i/f_{i0}=1$ , returns a very good approximation of the ultimate load, if compared with the FE model and the theoretical shear strength.

## 6. Non-linear static analyses of the entire church

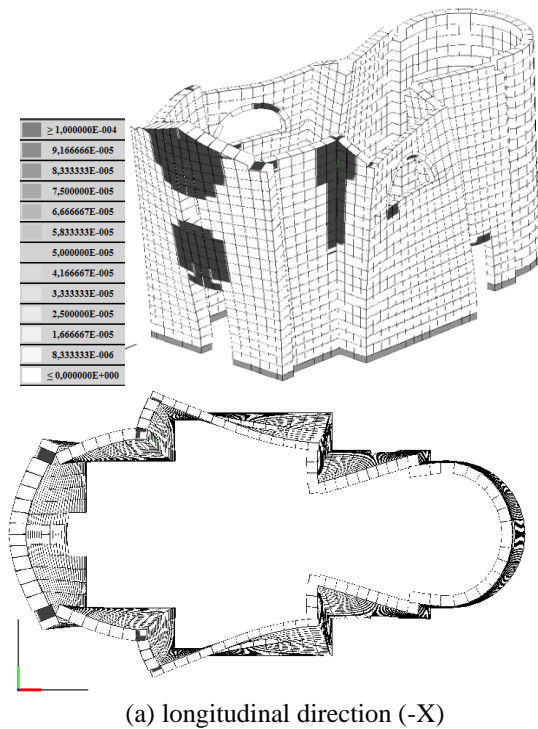
This Section comments the results of non-linear static analyses for the two models. The masonry non-linear mechanical parameters are assumed according to the indications of the Italian regulations for existing buildings (NTC 2008, Explanatory circular n°617 2009), as summarized in Table 2. The parameters used in the numerical simulations of the concrete damaged plasticity model (adopted in the FE model) are displayed in Table 4,

while Table 5 reports the equivalent parameters for the discrete model. The analyses were performed along the longitudinal (X) and transversal (Y) directions by considering horizontal set loads proportional to the mass distribution. The arc-length method was used in order to follow the softening behavior related to the assumed fracture energy.

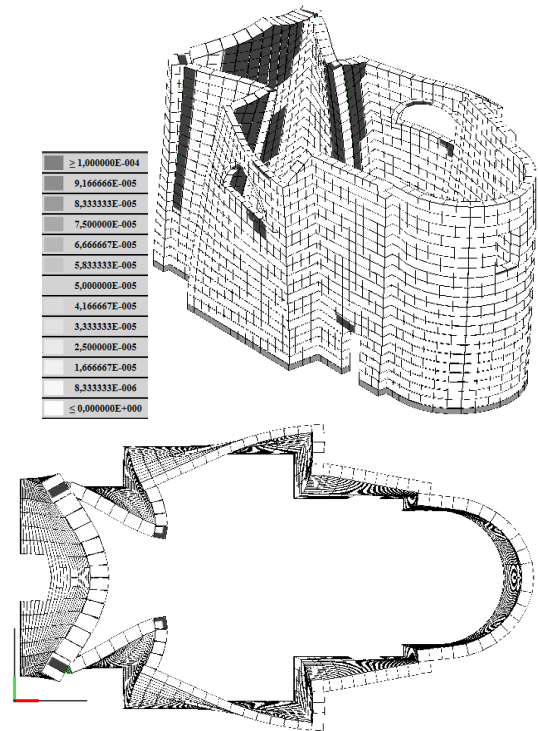
The concrete damage plasticity model, implemented in the FE model, requires the definition of the elastic modulus  $E$ , tensile and compressive strength  $f_t$  and  $f_c$  respectively, the corresponding fracture energies  $g_t$  and  $g_c$ , the ultimate deformation  $\epsilon_{umax,c}$ , the dilation angle  $\psi$ , the ratio of initial equi-biaxial compressive yield stress to initial uniaxial compressive yield stress  $f_{b0}/f_{c0}$  and the ratio of the second stress invariant on the tensile meridian to that on the compressive meridian  $K_c$ . All the parameters considered in the continuous model are summarized in Table 4.

The corresponding non-linear parameters, used for the discrete model, are computed according to the indications reported in Section 5 (see Table 5). In particular the diagonal shear behaviour is governed by the module  $G$ , the shear strength with zero axial compression  $f_{v0}$ , corresponding to the Turnsek-Cacovic yielding criterion, and the ultimate shear deformation  $\gamma_u$ . The sliding shear mechanism, between the panels along the connecting interfaces, has been ignored since in this typology of masonry the shear collapse is governed by the shear-diagonal response.

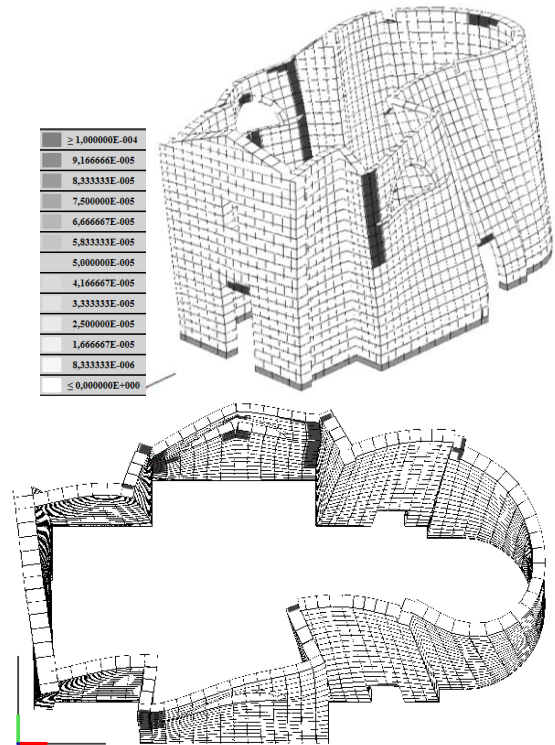
The results reported in Fig. 17 show the collapse mechanism of discrete model subjected to non-linear static analyses. Namely, Fig. 17(a) and Fig. 17(b) report the collapse scenarios related to the longitudinal directions,



(a) longitudinal direction (-X)



(b) longitudinal direction (+X)

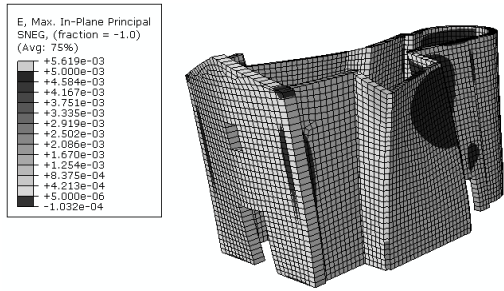


(c) transversal direction (Y)

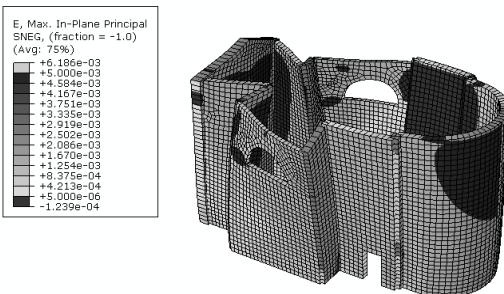
Fig. 17 Continued

Fig. 17 Mesh deformation at the peak load step of the analysis - HiStrA model

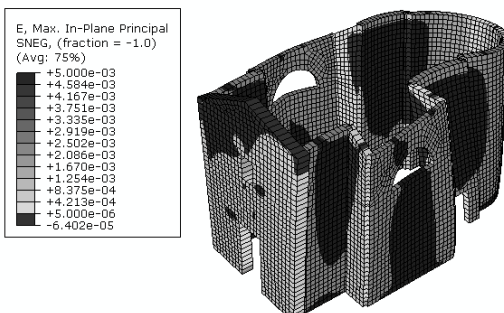
while Fig. 17(c) refers to the transversal direction. In this latter case a single analysis has been performed due to the symmetry of the model. In the pictures, the damage distributions are represented in terms of cumulative normal plastic deformations along the interfaces according to a grey scale representation.



(a) longitudinal direction (-X)

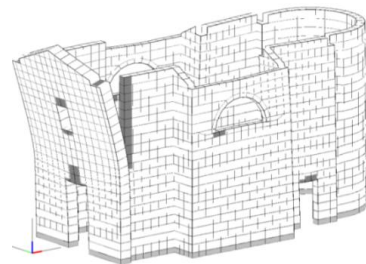


(b) longitudinal direction (+X)

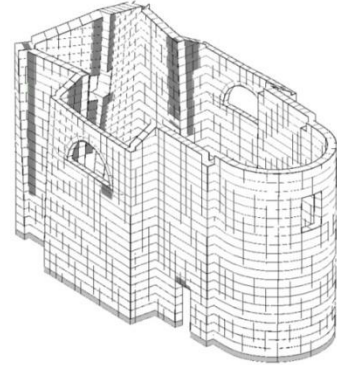


(c) transversal direction (Y)

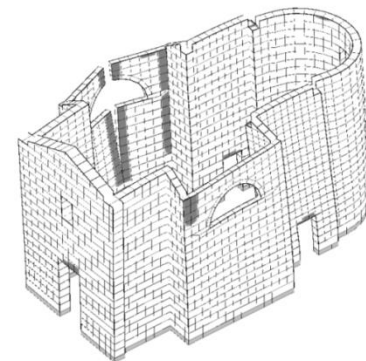
Fig. 18 Mesh deformation at the peak load step of the analysis - ABAQUS model



(a) longitudinal direction (-X)



(b) longitudinal direction (+X)



(c) transversal direction (Y)

Fig. 19 Mesh deformation at the last step of analysis - HiStrA model

Table 4 Non-linear parameters adopted for the finite element model (concrete damaged plasticity model)

$E$	$G$	$f_c$	$\epsilon_{umax,c}$	$f_t$	$g_t$	$\psi$	$f_{b0}/f_{c0}$	$K_c$
[MPa]	[MPa]	[MPa]	[-]	[MPa]	[N/mm]	[°]	[-]	[-]
1200	480	2.40	0.003	0.06	0.015	20	1.16	0.667

Table 5 Nonlinear parameters adopted for the discrete macro-model

$E$	$f_c$	$f_t$	$g_c$	$g_t$	$G$	$f_{v0}$	$\gamma_u$
[MPa]	[MPa]	[MPa]	[N/mm]	[N/mm]	[MPa]	[MPa]	[%]
1200	2.40	0.06	1.5	0.015	480	0.06	0.4

Fig. 18 reports the corresponding mechanisms and the relative damage distribution, obtained by the FE model. By comparing Fig. 17 to Fig. 18, a very good agreement can be observed between the continuous model and the discrete model, in terms of collapse mechanisms, for all the directions investigated. The damage distributions obtained by means of the discrete model are consistent to the results

obtained by the continuous FEM model.

A higher concentration of the damage is observed in the discrete model, where the plastic deformations are more concentrated in the intersection zones than the finite element model. This behaviour is probably more consistent to reality due to the discontinuous nature of the masonry. Both models provide results consistent to the typical collapse mechanisms of such structures when subjected to earthquake loads. Fig. 19 shows the collapse mechanisms obtained by the discrete model when the residual strength of the system has been reached. The final collapse of the façade is characterized by the detachment of the upper part at the connection with the orthogonal walls, when subjected to out of plane action forward directed. On the contrary, when the model is subjected to inward forces, a central vertical hinge characterizes the collapse mechanism of the main façade. It is worthy to notice that the discrete element modeling approach returns a complete set of collapse mechanisms, where the well known typical façade mechanism of monumental structures, characterized by an high rigid body component, are recognizable.

The results are reported in terms of push-over curves expressed with reference to different control points as depicted in Fig. 20. Ten control points have been

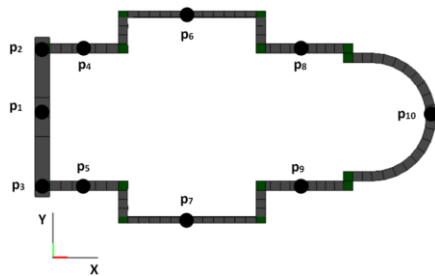
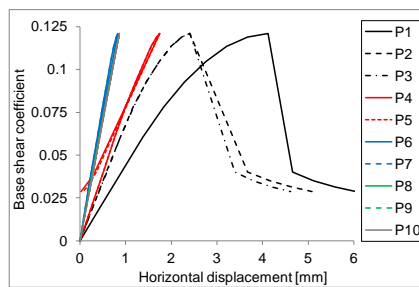
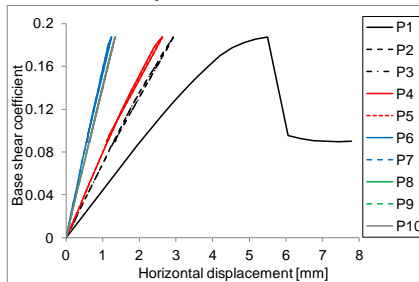


Fig. 20 Plan of the church with the disposition of the control points

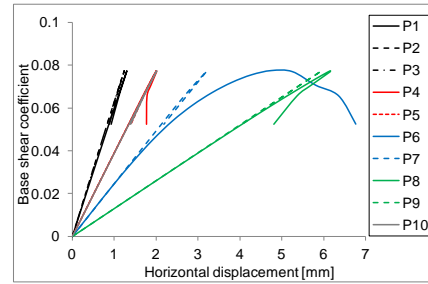


(a) analysis in -X direction

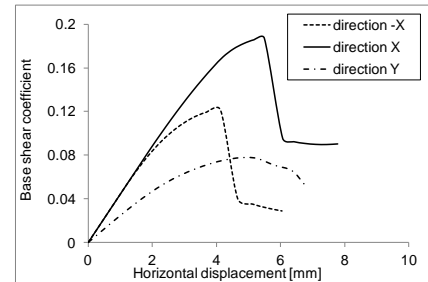


(b) analysis in +X direction

Fig. 21 Capacity curves - HiStrA model

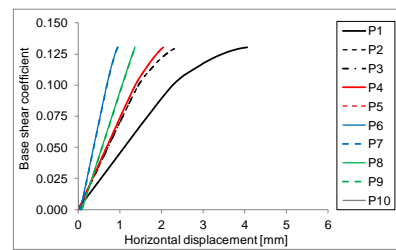


(c) analysis in Y direction

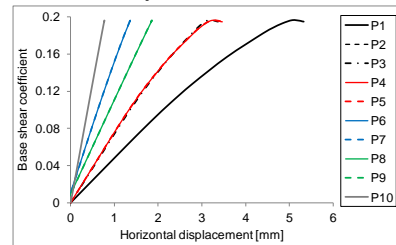


(d) maximum displacement for each direction

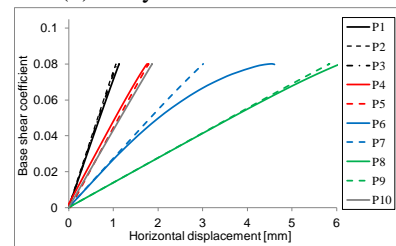
Fig. 21 Continued



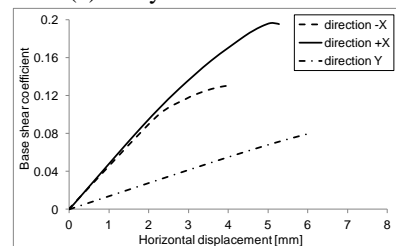
(a) analysis in -X direction



(b) analysis in +X direction



(c) analysis in Y direction



(d) maximum displacement for each direction

Fig. 22 Capacity curves - ABAQUS model

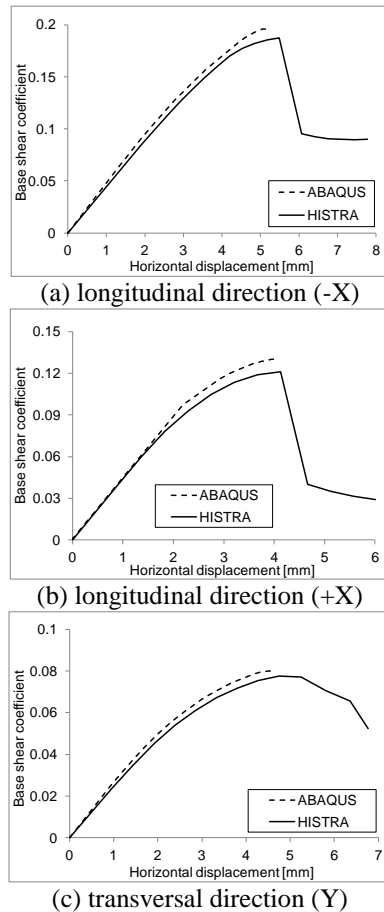


Fig. 23 Comparisons between the HiStrA and the ABAQUS in terms of capacity curves

considered, corresponding to different positions of the roof level of the church, with the aim to identify the different behavior of the different perimeter walls, in plane direction and out of plane direction.

Fig. 21 and Fig. 22 display the capacity curves obtained in HiStrA and ABAQUS models respectively. The base shear coefficient, given by the sum of reaction forces in horizontal direction with respect to the church self-weight, has been expressed as a function of the horizontal displacement of the chosen control points for both the investigated directions.

By comparing the results obtained by the two different approaches, it can be noticed how the discrete-model is able to catch the softening behaviour of the longitudinal response for the control points located near the main façade, being the first element, along the perimeter, that reaches the out of plane collapse.

The structure is, as expected, more flexible in the transversal direction than in the longitudinal direction. The transversal direction is where the minimum peak capacity is attained, equal to about 0.08 (Fig. 21(c) and Fig. 22(c)) against a maximum value of 0.19 related to the +X longitudinal analysis corresponding to the case in which the façade is pushed against the transverse walls (Fig. 21(b) and Fig. 22(b)). The case corresponding to the out-of plane façade mechanism, Fig. 21(a) and Fig. 22(b), is

characterized by a base shear coefficient of 0.12 for both the considered models.

Aiming at a better comparison between the two considered approaches, in Fig. 23 the capacity curves relative to the portion of the perimeter walls that exhibits the maximum displacement are compared.

An excellent correspondence is recognized both in terms of initial stiffness and maximum capacity. The analyses performed in the HiStrA are also characterized by the presence of the softening branch providing further information in terms of post peak behaviour.

It is worthy to notice that the results here reported and the relationship between the two modeling approaches are based on a linearized kinematics. This formulation is not able to catch the phenomena associated to the changing of the initial geometrical configuration and the high displacements amplitude, such as the  $P-\delta$  effects. Additionally, in the simulations masonry is considered as a monolithic solid through the thickness, without considering the possible disaggregation of the masonry texture. This failure mechanism, often observed in low-quality or in multi-leaf masonry, can cause very brittle partial structural collapses, during seismic events, that are neglected by the finite element model or the discrete macro-model here investigated.

## 7. Validation of the proposed model by considering real damages

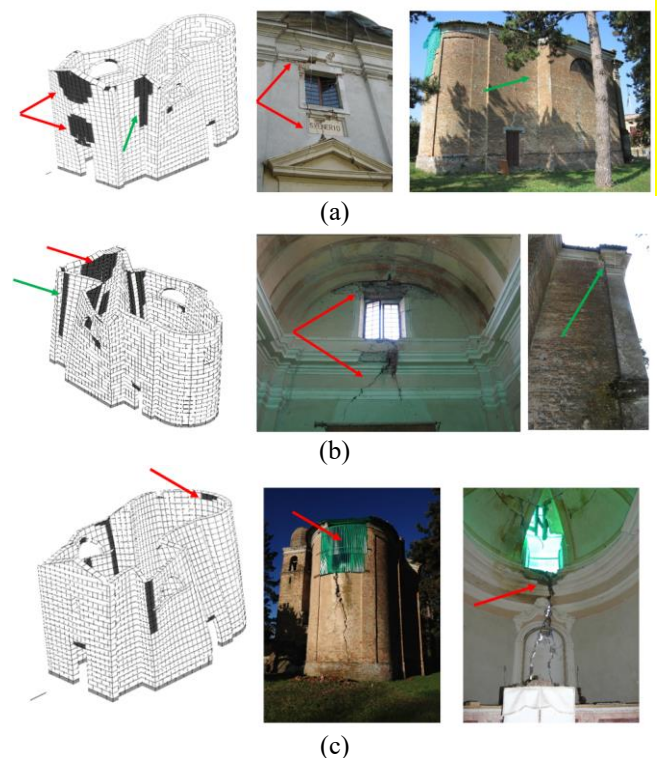


Fig. 24 Validation of the HiStrA model through the real damages occurred in St. Venerio's church: damages at the spandrel beams and detachment of side vertical wall (a); incipient overturning of the main façade (b); incipient overturning of the apse wall (c)

It is worthy to notice that the damages actually occurred in the church during the two main seismic shocks correspond to those suggested by the pushover analysis. Indeed, a comparison with the HiStrA model showed that the failures in the main façade (specifically, along the masonry spandrels adjacent to the rectangular window) are correctly reproduced by the model (red arrows in Fig. 24(a), (b)). In addition, the incipient detachment of the vertical walls of the side chapels is determined in the model as actually observed (green arrow in Fig. 24(a)). The main façade (green arrow in Fig. 24(b)) exhibited an incipient motion out-of-plane, as indicated by the vertical crack from the top of the wall up to about one-third of the total wall height. Finally, the model also reveals the failure observed in the apse wall. In the real situation, this latter failure appears more pronounced. This is probably due to the fact that it was present before the earthquake, as demonstrated by a plaster stripe of different color in the wall (Fig. 24(c)). These aspects confirm the reliability of both numerical models in the simulation of the seismic response of the church.

## 8. Conclusions

A macro-model approach, recently proposed by Pantò *et al.* (2016) is used, and critically compared with a standard continuous finite element model, with the aim of highlighting the advantages and the limits of the two modelling approaches. Both approaches have been shown to be effective for the seismic assessment of monumental structures, being able to provide comparable and realistic results.

A single-nave church, severely damaged during the 2012 Italian earthquake, has been analyzed by considering the discrete macro-element approach, implemented in the software HiStrA (Historical Structures Analysis 2015), and a finite element model implemented in the well known software ABAQUS (Simulia Abaqus 2012).

The comparisons were first performed in terms of linear modal analysis and then by non-linear push-over analyses. The linear comparison showed a surprising agreement in terms of mode shapes and vibration frequencies, although the adopted discretization approaches are different in terms of computational cost and numerical strategy.

In the non-linear context, the push-over analysis of the entire church provided an excellent correspondence both in terms of capacity curves and collapse mechanisms. The obtained results showed that the proposed discrete macro-model approach can be considered a reliable tool for the seismic assessment of churches. This model is particularly suitable for practical applications, being characterized by a lower computational cost of the typical non-linear FE models but providing comparable results.

## Acknowledgements

This research was carried out in the framework of DPC-RELUIS 2016, whose support is gratefully acknowledged.

The Authors wish to thank Eng.

Luciano Bellesia for providing information about the case study.

## References

- 3DMacro (computer program for the seismic assessment of masonry buildings), Release 3.0 (2014), Gruppo Sismica s.r.l., Catania, Italy, [www.3dmacro.it](http://www.3dmacro.it).
- Andreini, M., De Falco, A., Giresini, L. and Sassu, M. (2014), "Structural damage in the cities of Reggiolo and Carpi after the earthquake on May 2012 in Emilia Romagna", *Bull. Earthq. Eng.*, **12**(5), 2445-2480.
- Araujo, A., Lourenço, P.B., Oliveira, D. and Leite, J. (2012), "Seismic assessment of St James Church by means of pushover analysis - before and after the New Zealand earthquake", *Open Civ. Eng. J.*, **6**, 160-172.
- Asteris, P.G., Chronopoulos, M.P., Chrysostomou, C.Z., Varum, H., Plevris, V., Kyriakides, N. and Silva, V. (2014), "Seismic vulnerability assessment of historical masonry structural systems", *Eng. Struct.*, **62-63**, 118-134.
- Barbieri, G., Biolzi, L., Bocciarelli, M., Fregonese, L. and Frigeri, A. (2013), "Assessing the seismic vulnerability of a historical building", *Eng. Struct.*, **57**, 523-535.
- Betti, M. and Vignoli, A. (2008), "Assessment of seismic resistance of a basilica-type church under earthquake loading: Modelling and analysis", *Adv. Eng. Soft.*, **39**(4), 258-283.
- Betti, M. and Vignoli, A. (2011), "Numerical assessment of the static and seismic behaviour of the basilica of Santa Maria all'Impruneta (Italy)", *Construct. Build. Mater.*, **25**(12), 4308-4324.
- Caddemi, S., Caliò, I., Cannizzaro, F., Occhipinti, G. and Pantò, B. (2015), "A parsimonious discrete model for the seismic assessment of monumental structures", *Proceedings of the 15th International Conference on Civil, Structural and Environmental Engineering Computing*, Prague, Czech Republic, September.
- Caddemi, S., Caliò, I., Cannizzaro, F. and Pantò, B. (2014), "The seismic assessment of historical masonry structures", *Proceedings of the 14th International Conference on Civil, Structural and Environmental Engineering Computing*, Naples, Italy, September.
- Caliò, I., Marletta, M. and Pantò, B. (2012), "A new discrete element model for the evaluation of the seismic behaviour of unreinforced masonry buildings", *Eng. Struct.*, **40**, 327-338.
- Caliò, I. and Pantò, B. (2014), "A macro-element modelling approach of Infilled Frame Structures", *Comput. Struct.*, **143**, 91-107.
- Casapulla C. (2015), "On the resonance conditions of rigid rocking blocks", *Int. J. Eng. Technol.*, **7**(2), 760-771.
- Casapulla, C. and Argiento, L.U. (2016), "The comparative role of friction in local out-of-plane mechanisms of masonry buildings. Pushover analysis and experimental investigation", *Eng. Struct.*, **126**, 158-173.
- Casapulla, C., Jossa, P. and Maione, A. (2010), "Rocking motion of a masonry rigid block under seismic actions: a new strategy based on the progressive correction of the resonance response", *Ingegneria Sismica*, **27**(4), 35-48.
- Casolo, S. and Sanjustb, C.A. (2009), "Seismic analysis and strengthening design of a masonry monument by a rigid body spring model: the "Maniace Castle" of Syracuse", *Eng. Struct.*, **31**(7), 1447-1459.
- Dogliani, F., Moretti, A. and Petrini, V. (1994), *Le Chiese e i Terremoti* (in Italian), Lint Ed., Trieste, Italy.
- De Luca, A., Giordano, A. and Mele, E. (2004), "A simplified

- procedure for assessing the seismic capacity of masonry arches”, *Eng. Struct.*, **26**(13), 1915-1929.
- Explanatory circular 617 (2009), Istruzioni per l’applicazione delle nuove norme tecniche per le costruzioni di cui al D.M. 14.01.2008 (in Italian, Italian Minister for Infrastructures).
- Giresini, L. and Sassu, M. (2016), “Horizontally restrained rocking blocks: evaluation of the role of boundary conditions with static and dynamic approaches”, *Bull. Earthq. Eng.*, **15**(1), 385-410.
- Giresini, L., Fragiacomò, M. and Sassu, M. (2016), “Rocking analysis of masonry walls interacting with roofs”, *Eng. Struct.*, **116**, 107-120.
- Giresini, L. (2015), “Energy-based method for identifying vulnerable macro-elements in historic masonry churches”, *Bull. Earthq. Eng.*, **14**(3), 919-942.
- Heyman, J. (1999), *The Stone Skeleton: Structural Engineering of Masonry Architecture*, Cambridge University Press, Cambridge, United Kingdom.
- HiStrA (Historical Structure Analysis), release 17.2.3 (2015), HiStrA s.r.l, Catania, Italy, [www.histra.it](http://www.histra.it)
- Lourenço, P.B., Krakowiak, K.J., Fernandes, F.M. and Ramos, L.F. (2007), “Failure analysis of Monastery of Jerónimos, Lisbon: How to learn from sophisticated numerical models”, *Eng. Fail. Anal.*, **14**(2), 280-300.
- Lourenço, P.B., Mendes, N., Ramos, L. and Oliveira, D. (2011), “On the analysis of masonry structures without box behavior”, *Int. J. Arch. Herit.*, **5**(4), 369-382.
- Lourenço, P.B., Ramos, L.F., Vasconcelos, G. and Pena, F. (2008), “Monastery of Salzedas (Portugal): Intervention in the cloister and information management”, in *Structural Analysis of Historic Construction*, D’Ayala & Fodde eds., Taylor & Francis Group, London, United Kingdom.
- Lourenço, P.B., Trujillo, A., Mendes, N. and Ramos, L.F. (2012), “Seismic performance of the St. George of the Latins church: Lessons learned from studying masonry ruins”, *Eng. Struct.*, **40**, 501-518.
- Lourenço, P.B., Vasconcelos, G. and Ramos, L.F. (2001), “Assessment of the stability conditions of a Cistercian cloister”, *Proceedings of the 2nd International Congress Studies in Ancient Structures*, Istanbul, Turkey, July.
- Marques, R. and Lourenço, P.B. (2011), “Possibilities and comparison of structural component models for the seismic assessment of modern unreinforced masonry buildings”, *Comput. Struct.*, **89**(21), 2079-2091.
- Marques, R. and Lourenço, P.B. (2014), “Unreinforced and confined masonry buildings in seismic regions: Validation of macro-element models and cost analysis”, *Eng. Struct.*, **64**, 52-67.
- Mendes, N. and Lourenço, P. (2010), “Seismic assessment of masonry “Gaioleiros” buildings in Lisbon, Portugal”, *J. Earthq. Eng.*, **14**(1), 80-101.
- Milani, G. and Valente, M. (2015a), “Failure analysis of seven masonry churches severely damaged during the 2012 Emilia-Romagna (Italy) earthquake: non-linear dynamic analyses vs conventional static approaches”, *Eng. Fail. Anal.*, **54**, 13-56.
- Milani, G. and Valente, M. (2015b), “Comparative pushover and limit analyses on seven masonry churches damaged by the 2012 Emilia-Romagna (Italy) seismic events: possibilities of non-linear finite elements compared with pre-assigned failure mechanisms”, *Eng. Fail. Anal.*, **47**, 129-161.
- Moropoulou, A., Polikreti, K., Ruf, V. and Deodatis, G. (2003), “San Francisco Monastery, Quito, Ecuador: characterisation of building materials, damage assessment and conservation considerations”, *J. Cultural Herit.*, **4**(2), 101-108.
- NTC - Decree containing the new Building Code (Norme Tecniche per le Costruzioni - in Italian) (2008), published on the Official Gazette no. 29, Italian Minister for Infrastructures.
- Pantò, B., Cannizzaro F., Caddemi, S. and Calìo, I. (2016), “3D macro-element modelling approach for seismic assessment of historical masonry churches”, *Adv. Eng. Soft.*, **97**, 40-59.
- Rovero, L., Alecci, V., Mechelli, J., Tonietti, U. and De Stefano, M. (2016), “Masonry walls with irregular texture of L’Aquila (Italy) seismic area: validation of a method for the evaluation of masonry quality”, *Mater. Struct.*, **49**(6), 2297-2314.
- Simulia Abaqus CAE 6.12 (2012), User’s and Theory Manuals, Dassault Systèmes.

AG